Supplementary Information for:

On-chip hybrid plasmonic light steering concentrator with ~ 96% coupling efficiency

Tian Zhang,[a] Maoning Wang,[a] Yong Yang,[a] Fei Fan,[a] Takhee Lee,[b] Haitao Liu[a] and Dong Xiang*[a]

[a]Institute of Modern Optics, Nankai University, Key Laboratory of Optical Information Science and Technology, Ministry of Education, Tianjin 300350, China

[b]Department of Physics and Astronomy, and Institute of Applied Physics, Seoul National University, Seoul 08826, Korea

*Corresponding author. Email: xiangdongde@126.com

S1. Description of the material

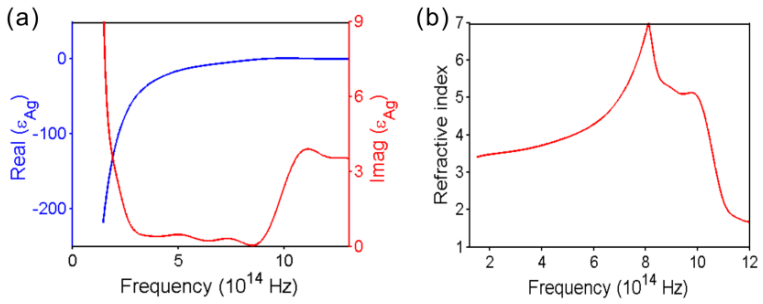

Figure S1 (a) The real and imaginary parts of the permittivity of silver are obtained by polynomial fitting of the experimental data provided by Johnson and Christy.[1] (b) The refractive index of silicon obtained by fitting the data from Green.[2]

S2. Coupling between the silver strips

In order to understand the coupling mechanism between multiple silver strips, we first analyse the mode of a single silver strip in free space. Figure S2(a) shows the dispersion of the three lowest modes of rectangular silver strip. The dispersion properties of the SPPs mode are characterized by the complex propagation constant β and frequency. As shown in Figure S2(b), based on the electric-displacement distribution and the time-averaged power flow distribution for each mode, we label these modes TM_0, TE_1 and TE_2. These primary modes are perfectly symmetrical and each mode has a different working window. Unlike the mode TE_1, which has a continuous working window, the TM_0 mode has two empty windows (i.e., 0.484PHz ~ 0.577PHz, 0.599PHz ~ 1.038PHz). The TE_2

mode has only a radiation mode, which is different from the mode with total-level working window (bound mode, forbidden band, radiation mode). Therefore, for the design of nanophotonics devices, the selection of working window is crucial.

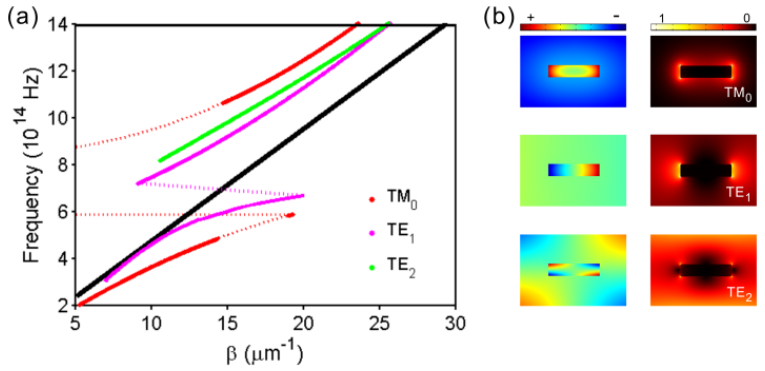

Figure S2 (a) The dispersion relationship of the three lowest order modes of rectangular silver strip in free space, where the black line represents the light line in air. (b) Normalized electric-displacement distribution (left) and time-averaged power flow distribution (right) of the three lowest order modes. Top to bottom: TM_0 (0.484PHz), TE_1 (0.309PHz), TE_2 (0.845PHz).

The mediation of the silicon substrate changes the primary modes with perfect symmetry in free space into quasi-modes (denoted q-TM_0, q-TE_1, q-TE_{-1}, q-TE_2) with partial symmetry. Moreover, these quasi-modes generate a series of new hybridized modes (denoted HTM_1, HTM_2, HTE_1 and HTE_2) at a specific frequencies based on the substrate effect. As shown in Figure S3(a), we have fully characterized the dispersion relationship for each mode of silver strips supported by a silicon substrate over a relatively wide range of frequencies. It can be found that the quasi-modes and the hybridized modes cannot exist simultaneously at the same frequency. Therefore, the new hybridized modes can be regarded as the result of mutual coupling between quasi-modes under different working windows. Figure S3(b) shows the normalized electric-displacement distribution (left) and the time-averaged power flow distribution (right) of the four quasi-modes that lose perfect symmetry. As shown by Zhang *et al.*,[3] the substrate effect can be qualitatively interpreted using an "image charge" picture in the quasi-static limit.[4] Figure S3(c) illustrates schematically the coupling between the primary quasi-modes with the same frequency. The new hybridized modes HTM_1 and HTM_2 are generated by the in-phase coupling (inducing the same polarized charges on the substrate surface as the primary mode) and out-of-phase coupling (canceling their induced polarized charges on the substrate surface) between q-TM_0 and q-TE_{-1} modes, respectively. The same is true for the generation of hybridized modes HTE_1 and HTE_2. The red negative charge in the figure is induced by the positive charge in the metal. The frequency required for coupling depends on the shape and size of the plasmonic structure and the permittivity of the substrate. The calculation results of four hybridized modes shown in Figure S3(d) coincide with the analysis in Figure S3(c), confirming the validity of the coupling mechanism.

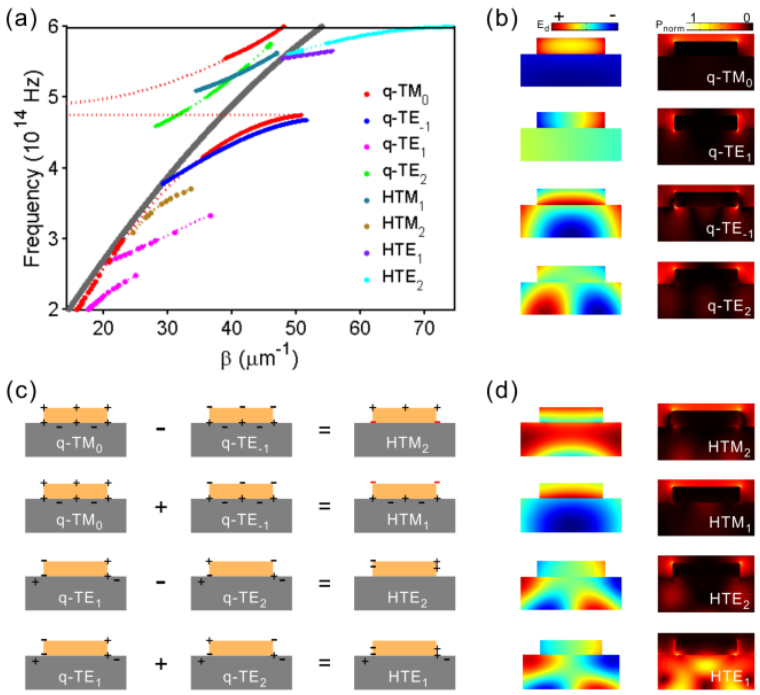

Figure S3 Substrate-mediated coupling. (a) The dispersion relationships of four quasi-modes and four hybridized modes of rectangular silver strips on silicon substrate, where the gray line represents the light line in silicon. (b) Normalized electric-displacement distribution (left) and time-averaged power flow distribution (right) of the four quasi-modes. Top to bottom: q-TM_0 (0.224PHz), q-TE_1 (0.201PHz), q-TE_{-1} (0.385PHz), q-TE_2 (0.508PHz). (c) Schematic drawing of coupling between primary quasi-modes based on the substrate effect. The red negative charge in the figure is induced by the positive charge in the metal. (d) Normalized electric-displacement distribution (left) and time-averaged power flow distribution (right) of the four hybridized modes. Top to bottom: HTM_2 (0.337PHz), HTM_1 (0.517PHz), HTE_2 (0.555PHz), HTE_1 (0.551PHz).

For the HPP structure, coupling can take place between each silver strip under the mediation of a silicon substrate. From the dispersion relationship in Figure S3(a), for the silver strip supported by the silicon substrate, there are two independent quasi-modes (q-TM_0 and q-TE_1) at the frequency of 0.2 PHz. According to the "image charge" picture, as shown in Figure S4(a), two supermodes (symmetric modes S_1, S_2) can be generated by the in-phase coupling (inducing the same polarized charges on the substrate surface) between them. Figure S4(b) shows the normalized electric-field distribution for the symmetric modes (S_1 and S_2) consistent with the meaning of the charge map, confirming our understanding of the coupling mechanism. For the HPP structure with N ($N \geq 3$) silver strips, (N+1) supermodes can be generated according to the substrate effect. However, the more modes are generated, the greater loss for a system that has a specific mode requirement.

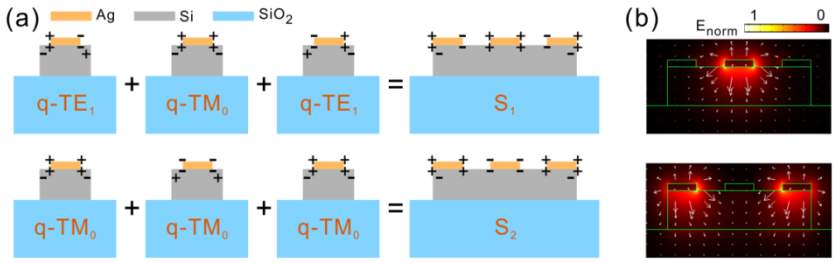

Figure S4 (a) Schematic drawing of substrate-mediated coupling between silver strips. (b) Normalized electric-field distribution for two symmetric supermodes (S_1 and S_1).

S3. Loss mode and back reflection

The presence of the top silver plate greatly reduces the coupling length of the hybrid photonic-plasmonic (HPP) sandwich structure and improves the coupling efficiency, but at the same time it also introduces an additional loss mode A_L. Meanwhile, the back reflection is also an important factor in reducing the coupling efficiency during coupling process of the device. In this paper, we use the power ratio (Γ_{A_L} and Γ_R) calculated by the time-averaged Poynting vector[5] to illustrate the influence of their respective proportions on the coupling efficiency. The power ratio Γ_m is defined as $\Gamma_m = P_m / P_t$, where P_m is the power of the mode considered, P_t is the total incident power. As shown in Figure S5, the results show that the proportion of the loss mode first decreases and then increases with the increase of the thickness of silver plate. Similarly, the calculated back reflection ratio Γ_R also follows the same trend, except that the proportion of loss mode is the smallest at a thickness of 20 nm. However, since the loss mode is mainly responsible for the loss, the loss of the device is minimal at the thickness of 30nm.

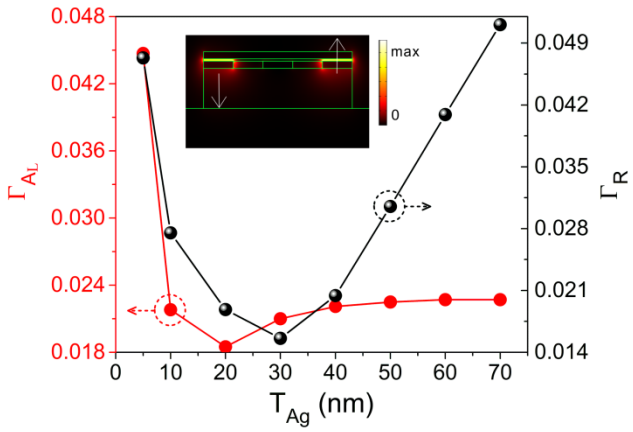

Figure S5 (a) The relation between the power ratio Γ_{A_L} of loss mode A_L and the thickness of the top silver plate T_{Ag} in the HPP sandwich structure. Inset shows the electric-field distribution of loss mode A_L. (b) The dependence of the back reflection ratio Γ_R in the silicon waveguide on the thickness of the plate during the coupling process.

References

1. P. B. Johnson and R. W. Christy, *Phys. Rev. B*, 1972, **6**, 4370–4379.
2. M. A. Green, *Sol. Energ. Mat. Sol. Cells*, 2008, **92**, 1305-1310.
3. S. P. Zhang and H. X. Xu, *ACS Nano*, 2012, **6**, 8128-8135.
4. K. C. Vernon, A. M. Funston, C. Novo, D. E. Gómez, P. Mulvaney and T. J. Davis, *Nano Lett*., 2010, **10**, 2080-2086.
5. J. D. Jackson, Classical Electrodynamics, Wiley & Sons, New York, 1975.